Modeling DelftaCopter from Flight Test Data

Meulenbeld, Joost; de Wagter, Christophe; Remes, Bart

Modeling DelftaCopter from Flight Test Data

J.F. Meulenbeld,* C. De Wagter,† B.D.W. Remes
Delft University of Technology, Kluyverweg 1, 2629HS Delft, the Netherlands

ABSTRACT

The DelftaCopter, a tilt-body tailsitter UAV, endures large gyroscopic moments due to the single helicopter rotor providing its thrust. In previous research by de Wagter et al.[1] the DelftaCopter's attitude dynamics were modeled using a rigid rotor, as is customary for small helicopter modeling. A controller based on this model was unable to compensate coupling between pitch and roll rate caused by gyroscopic moments.

In this paper, two models are compared for reproducing the attitude dynamics of the DelftaCopter in hover. The Cylinder Dynamics (CD) model, used in the previous research, assumes a rigid rotor. The Tip-Path Plane (TPP) model incorporates flapping motion of the blades and was developed by Mettler[2]. The two models are compared by fitting each model's parameters on flight data using chirps, sine waves with increasing frequency, as system identification maneuvers. The TPP model is shown to be much more accurate in reproducing the high-frequency attitude dynamics. An LQR controller directly based on the TPP model is shown to yield adequate tracking performance. This validates the applicability of this model to the DelftaCopter.

For forward flight, an extension to the TPP hover model is proposed incorporating the aerodynamics of the wings and elevons. It is shown that with the extension, chirps in forward flight can be simulated with reasonable accuracy. This paves the way for a model-based controller in this flight state.

1 INTRODUCTION

While Unmanned Aerial Vehicles (UAVs) have been around for many years, reaching a large endurance and range on small platforms remains a challenge. The Outback Medical Challenge encourages research on UAVs with the capability of long-distance flights and landing in rough terrain. This requires vertical take-off and landing (VTOL). There are multiple concepts for combining long range and VTOL, of which a qualitative comparison is given by Herbst et al.[3] One of the concepts is the tail-sitter or tilt-body hybrid UAV. This concept has its rotors pointed upwards in hover mode, but can tilt downward by 90° to transition to forward flight. In forward flight the wings of the UAV provide the required lift for level flight, which is more efficient than using rotors for lift. The transition is shown in Figure 1.
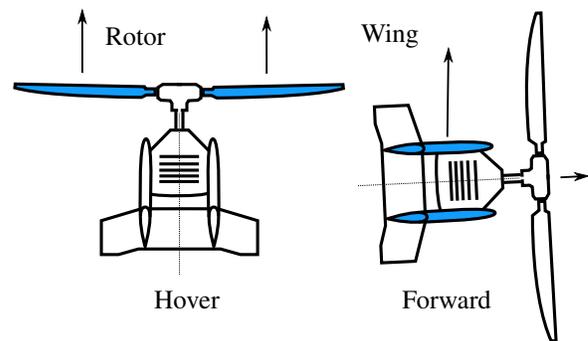

Figure 1: Transition of the DelftaCopter.

Within the class of tilt-body UAVs, the amount of rotors varies. Using four rotors allows to use standard quadcopter control methods in hover, while taking into account aerodynamic forces in forward flight. Examples of this class are the VertiKUL[4] and Quadshot[5]. Two rotor systems have either counter-rotating in-line rotors like the Vertigo[6] or a combination of two rotors that rotate in the same plane, like the MAVIon[7] or Cyclone[8]. Both options use aerodynamic surfaces for control. The single-rotor tilt-body UAV concept is implemented by the DelftaCopter[9] and the Flexrotor, developed by a commercial company[1]. This makes the DelftaCopter a unique platform for researching single-rotor tilt-body UAVs.

The DelftaCopter has been designed and built for the Outback Medical Challenge in 2016 by the DelftaCopter team at TU Delft[9]. In 2018, the new competition again requires a flight of $\approx 60\,\mathrm{km}$ in one hour, landing in rough terrain halfway[10]. This demands a UAV that has a long range and speed, and can do VTOL. The efficiency advantage of a single rotor over four rotors is why this concept was chosen. The DelftaCopter is shown in Figure 2.

Though the single rotor providing thrust and lift is more efficient than a design with multiple rotors, it yields certain control challenges. As for most helicopters, the gyroscopic effect plays an important role in the dynamics of the DelftaCopter. Contrary to most helicopters, the inertia of the fuse-

---

*joost.meulenbeld@gmail.com
†C.deWagter@tudelft.nl

[1]http://aerovel.com/

Figure 2: DelftaCopter in hover. In forward flight, the entire fuselage pitches down $90°$ and the rotor provides the thrust as shown in Figure 1.

lage underneath the rotor is quite large compared to the rotor inertia. Often helicopters are controlled with the assumption that an applied roll moment yields a pitch rate and vice versa. This is the case when no bulky fuselage is present under the rotor[11] and the response resembles that of a pure gyroscope. The DelftaCopter has a heavy fuselage due to the long wings and electronics placed at the wing tips for better radio reception. This also makes the inertia much larger in the roll direction than in the pitch direction.

The currently used attitude rate controller was described by De Wagter and Smeur[1]. It uses proportional feedback on the rotational rate error. Additionally, it tries to compensate pitch and roll gyroscopic coupling using identified coupling magnitude $C_{q_{\dot{p}}}$ and $C_{p_{\dot{q}}}$ and another gain K_c. The formulation is given in Equation (1). δ_x is the roll command, δ_y pitch. G is the actuator effectiveness matrix, K_p and K_q are feedback gains, p is roll rate and q is pitch rate, and K_c is a tuning factor.

$$\begin{bmatrix} \delta_x \\ \delta_y \end{bmatrix} = G^{-1} \begin{bmatrix} K_p p_{err} + q C_{q_{\dot{p}}} K_c \\ K_q q_{err} + p C_{p_{\dot{q}}} K_c \end{bmatrix} \quad (1)$$

This controller relies on the model identified using flight data. The model is based on the assumption of a rigid rotor applying gyroscopic moments. The factor $K_c = 0.5$ in Equation (1) yielded the best results with little coupling between pitch and roll, while a value of 1 would be expected to work best if the underlying model is valid.[1] This indicates that the assumed model is incapable of producing all relevant attitude dynamics of the DelftaCopter. This leads to this paper's research question: What is the best model to replicate the attitude dynamics of the DelftaCopter for the purpose of control?

The research question was answered by comparing multiple models for their accuracy. The results are described in this paper as follows. Section 2 describes the models that are compared. To do this comparison, flight tests were performed and the models' parameter identified, as described in Section 4. With the fitted models, a controller was designed and imple-

mented for hover mode, the design and performance of which is shown in Section 5. In Section 6 an extension to the model is proposed to incorporate the effect of the wing aerodynamics during forward flight. Finally, in Section 7 the results are discussed and a conclusion is drawn with respect to the used models for the DelftaCopter.

2 IDENTIFICATION MODELING

For the purpose of modeling the DelftaCopter for control applications, a system identification model is to be chosen. Not all parameters in this model can be found from direct physical measurement, so a grey-box parameter estimation procedure was used that estimates the unknown parameters from flight data. The models used for this are described in this section.

3 DESCRIPTION OF MODEL TYPES

One of the important differences between the assumptions of different models is how they incorporate the flapping dynamics of the helicopter. The flapping dynamics of a helicopter are well covered in Bramwell's helicopter dynamics[12] as follows. The helicopter pitch and roll attitude are controlled by using the swashplate of the rotor. This device allows to set the variation of the blade pitch angle over the rotation of the rotor using collective (for thrust) and cyclic pitch (for attitude control). The blade pitch angle follows the relation below.

$$\theta = \theta_0 - \delta_x \cos \Psi - \delta_y \sin \Psi \quad (2)$$

In this equation taken from Bramwell's book[12, sec. 1.6.2], θ is the blade pitch angle, Ψ is the in-plane rotation of the blade from the back of the helicopter and θ_0 is the collective pitch angle determining the lift generated by the rotor. δ_x and δ_y are determined by the cyclic pitch setting of the (auto)pilot. This variation of pitch angle over the rotation will generate differences in aerodynamic forces which in turn makes the blade flap up and down. The following categories of models can be distinguished based on how they incorporate the flapping dynamics.

- The first and most elaborate approach is to deal with the flapping blade explicitly, including the flapping angle of every individual blade as a state of the model. This allows theoretical analysis into the response but also requires many physical parameters to be accurately measured. It leads to a model that is very hard to use for control design due to its time-dependence.

- An often applied simplification is to relate attitude dynamics to the Tip-Path Plane (TPP), i.e. the plane in which the tips of the rotor travel. It can be derived directly using the flapping angle equation shown in Equation (2). A mathematical description is derived by Mettler by neglecting high-frequency dynamics of the rotor.[2] The TPP is represented by two angles, a and b,

which indicate the angle between the TPP and the horizontal, in the longitudinal and lateral direction respectively, as shown in Figure 3. The TPP angles change under influence of control inputs, rotations of the fuselage and gyroscopic precession of the rotor. A moment is applied on the fuselage if the a and b angles are not zero, due to the effective spring between the rotor blade and axis and the offset of thrust application point on the rotor and the center of mass of the fuselage.[2, 13] This way, the rotor is a separate body from the fuselage with its own dynamics. This simplification is valid if the rotor rotational frequency ($\approx 1650\text{RPM} = 27.5\,\text{Hz}$ for the DelftaCopter) is much higher than the highest eigenfrequency of the body-TPP coupling dynamics ($\approx 5\,\text{Hz}$ for the DelftaCopter, as shown later). Then the oscillations of the rotor are damped out by the body dynamics and the forces can be expressed as an average over a rotation of the rotor. Mettler applies this type of model to a small unmanned helicopter, resulting in an accurate model that matches with flight data[2].

- The last simplification is to ignore the flapping dynamics and treat the rotor as a rigid object, with no flapping angle possible. This way, the gyroscopic effect that the rotor produces still affects the fuselage, but the time-dependent coupling between fuselage and rotor are eliminated. This method is used widely for small helicopters[14, 15, 16]. A TPP model can be transformed into a model without flapping dynamics by setting the derivatives of the a and b angles to zero, which is a valid simplification if the flapping dynamics are much faster than the fuselage dynamics[13]. The type of model without flapping dynamics will be called a cylinder dynamics (CD) model, since the gyroscopic effect of the rotor can be included by modeling it as a rigid rotating cylinder.

In this paper, the TPP and CD models are compared for their accuracy to replicate in-flight test data. The formulation for the TPP and CD model will be given below. Both are linear time-invariant models in state-space form, using the equations below.

$$\dot{\bar{x}} = A\bar{x} + B\bar{u} \tag{3}$$

$$\bar{y} = C\bar{x} + D\bar{u} \tag{4}$$

3.1 TPP model description

The Tip-Path plane (TPP) model has been adapted from Mettler's helicopter model, of which only the p, q, a and b states are used[2]. For the TPP model, the state vector is $\bar{x} = (p, q, a, b)^T$ and the input vector is $\bar{u} = (\delta_x, \delta_y)^T$. The state-space A, B and C matrices for the TPP model are given in Equations (5) to (7). The D-matrix consists of only zeros. The model has nine parameters that need to be found from flight testing: L_b and M_a represent the spring constants

of the Tip-Path Plane, consisting of both the stiffness of the blade and blade hinge, and the offset between rotor and center of mass of the fuselage. τ_{f_n} is the time constant of the TPP dynamics. A_{b_n} and B_{a_n} are cross-coupling terms that describe how the TPP interchanges the a and b angles over time. The four parameters in the B-matrix give the actuator effectiveness. Since the DelftaCopter may fly with different RPMs, the theoretical dependence of the parameters is made explicit: $\tau_f = \tau_{f_n}/\Omega$, $A_b = A_{b_n}/\Omega^2$ and $B_a = B_{a_n}/\Omega^2$[2, sec. 2.3]. Section 4.3 comments on the validity of this dependence.
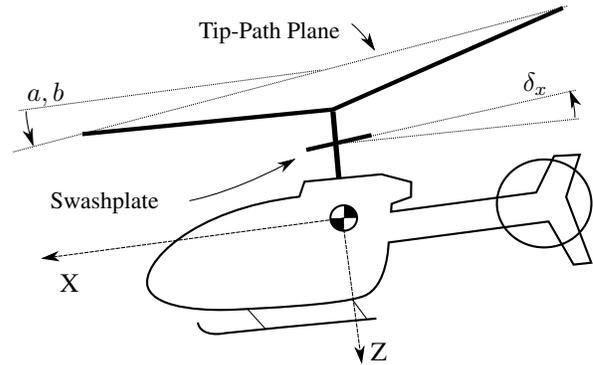

Figure 3: Helicopter Tip-Path plane (TPP) model. The axes shown in this image are as used in the DelftaCopter while it is in hover. The y-axis is chosen using the right-hand rule.

$$A_{TPP} = \begin{bmatrix} 0 & 0 & 0 & \text{L}_\text{b} \\ 0 & 0 & \text{M}_\text{a} & 0 \\ 0 & -1 & -\frac{\Omega}{\tau_{fn}} & \frac{\text{A}_{\text{b}_\text{n}}}{\Omega\,\tau_{fn}} \\ -1 & 0 & \frac{\text{B}_{\text{a}_\text{n}}}{\Omega\,\tau_{fn}} & -\frac{\Omega}{\tau_{fn}} \end{bmatrix} \tag{5}$$

$$B_{TPP} = \begin{bmatrix} 0 & 0 \\ 0 & 0 \\ \frac{\text{A}_{\text{lat}}\,\Omega}{\tau_{fn}} & \frac{\text{A}_{\text{lon}}\,\Omega}{\tau_{fn}} \\ \frac{\text{B}_{\text{lat}}\,\Omega}{\tau_{fn}} & \frac{\text{B}_{\text{lon}}\,\Omega}{\tau_{fn}} \end{bmatrix} \tag{6}$$

$$C_{TPP} = \begin{bmatrix} 1 & 0 & 0 & 0 \\ 0 & 1 & 0 & 0 \end{bmatrix} \tag{7}$$

3.2 CD model description

The state used in the Cylinder Dynamics (CD) model is $\bar{x} = (p, q)^T$, and the input is the same as for the TPP model. Both the A- and B-matrices consist of four identifiable parameters, as shown in Equations (8) and (9) below. All identifiable variables could be ascribed physical meaning as a steady-state solution of the a and b states in the TPP model, or through gyroscopic moments and aerodynamic damping. The latter option would entail measuring many different parameters including aerodynamic forces, and does not improve usefulness for control design since the final model has the same structure as it has now.

$$A_{cyl} = \begin{bmatrix} L_p & L_q \\ M_p & M_q \end{bmatrix} \qquad (8)$$

$$B_{cyl} = \begin{bmatrix} L_{lat} & L_{lon} \\ M_{lat} & M_{lon} \end{bmatrix} \qquad (9)$$

3.3 TPP and CD model equivalency

The a and b states of the TPP model can be regarded as the angular accelerations in q and p states respectively, i.e. the a state is directly related to the derivative of q. This means that instead of determining the angular acceleration directly using the control input as in the CD model, the angular acceleration has its own dynamics and is influenced by the control input.

The steady-state solution resulting from $\dot{a} = \dot{b} = 0$ in the TPP models allows substitution of steady-state a and b values in the $\dot{p}$ and $\dot{q}$ equations, which then yields a comparable system to the CD model, with every CD model parameter linked directly to a combination of parameters in the TPP model.[13]

3.4 Conclusion

The CD and TPP models will be fitted purely based on the input-output response. For the TPP model the a and b states are not measured, but result from the measurements of their interactions with the pitch and roll rates and actuators. This means that these states cannot directly be validated from measurements. The TPP model has but one parameter more than the CD model, but more importantly it has two more eigenfrequencies that should allow capturing a broader range of response frequencies.

4 FLIGHT TESTING AND SYSTEM IDENTIFICATION

For fitting the model parameters, flight tests were performed in an indoor environment. To make sure that the range of interesting dynamics is covered in every flight test, an automated flight testing procedure was developed. According to Tischler et al., the "chirp" maneuver is able to generate the required frequency content.[17] A chirp is a sine wave with a frequency increasing continuously over time. When a chirp is inserted in a single actuator, the system response shows the coupling between all axes and how this changes with frequency. Tischler also states that to get the best results, the system should be flown open-loop. However, this is not possible with the DelftaCopter due to the dynamics, so the attitude controller is still active during flight tests. To lower the coherence between different axes introduced by the controller, noise is added to every axis independently, as per Tischler's suggestion[17]. The noise is filtered with a first-order low-pass filter with the cut-off at the highest frequency of the chirp. An exponential-time chirp is used to have enough content at the lower frequencies.

The chirp signal is generated and added to the controller signal and the resulting actuator signal is stored with the gyroscope measurements on an SD-card at a frequency of $500\,\text{Hz}$. The chirp settings are given in Table 1. The frequency range starts and ends higher than suggested by Mettler[2]. The

lower frequency is limited by the size of the indoor facility in which the tests were performed, while the higher frequency now includes more of the high-frequency dynamics. The eigenfrequencies of the identified model are well within the range of the chirp.

Variable	Value
Start frequency	$0.5\,\text{Hz}$
End frequency	$10\,\text{Hz}$
Noise fraction	0.2
C_1	4
C_2	$\frac{1}{\exp{(C_1)}-1}$

Table 1: Settings used for the exponential-time chirp. The noise fraction is the ratio between the amplitude of the chirp and the standard deviation of the white noise that is filtered and added to the chirp signal. C_1 and C_2 are the values used in the exponential-time chirp formulation in the book by Tischler[17].

After flight testing, the data was filtered digitally by an ideal low-pass filter with a cut-off frequency of $15\,\text{Hz}$. This removes vibrations caused by the rotor which rotates at around $27.5\,\text{Hz}$. The input channels were centered around 0 to remove input bias. The resulting data streams were used to fit the parameters in the time domain using the MATLAB system identification toolbox.

4.1 Chirp results

The results for a roll chirp are shown in Figure 6. In this figure, the measured roll and pitch rates are shown for the online measurement, the simulated TPP model and simulated CD model. The pitch rate q is a result of the pitch-roll coupling introduced by the rotor. It is clear that the CD model is able to accurately simulate the response up to a certain frequency, but does not include the eigenfrequency which is excited at around $28.5\,\text{s}$. The TPP model does include this eigenfrequency and is much better at reconstructing the system response. This is due to the fact that the TPP dynamics model has four states, and therefore four eigenfrequencies. The two eigenfrequencies the TPP model has extra compared to the CD model lead to higher frequencies being accurately modeled as well. A pitch chirp is shown in Figure 7. In this chirp, the mismatch between the CD model and measurements is even worse.

4.2 Model fit validation

Figure 4 shows pitch and roll doublets, as flown by a pilot while the attitude controller was active. This flight data was not used for fitting the models and can thus be used as validation for model accuracy. Table 2 shows the eigenfrequencies of both the identified TPP and CD systems. The slower eigenfrequency corresponds to a pitch-roll coupled motion and is present in both models. The faster eigenfrequency is almost

purely pitch and is not present in the CD model. This explains why the pitch response of the CD model is so far off.
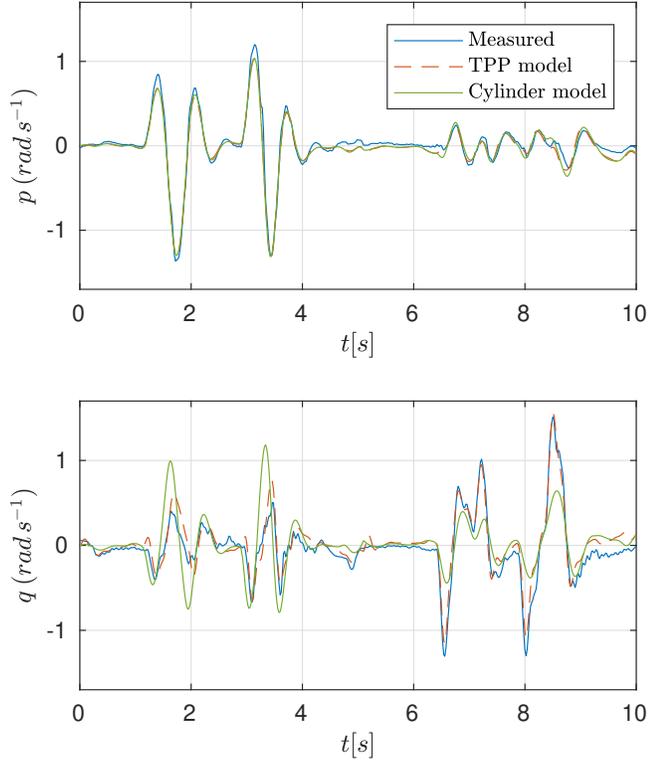

Figure 4: First some roll, then some pitch doublets, flown manually with the attitude controller active. While the roll response is quite accurately modeled by both models, the pitch response is much better in the TPP model. Since the CD model misses the higher eigenfrequency, the fast movements of the pitch are not accurately modeled. This difference is due to the low pitch inertia compared to the roll inertia.

The numerical difference between the measurements and the model output is given in Table 3. The Normalized Root Mean Squared Error (NRMSE) percentage is used as a measure of the goodness of fit, where 100% constitutes a perfect match. The NRMSE percentage is given in Equation (10), where y is the measured signal, $\hat{y}$ is the model output and $\bar{y}$ is the average of the measured signal. The fraction in Equation (10) is thus also equal to the root mean squared error divided by the standard deviation of the measurement.

$$NRMSE = 100\% \left(1 - \frac{||y - \hat{y}||}{||y - \bar{y}||}\right) \qquad (10)$$

The fitted parameters are shown in Table 4. The difference in roll and pitch inertia is apparent from the L_b and M_a values, which differ by a factor of 4.8. To validate that the parameters were not overfitted to a particular chirp, the TPP model was fitted to two different sets of chirp data and their fitted parameters were compared. The highest single change

	Pole	Frequency [Hz]	Damping [−]
CD model	1-2	1.54	0.35
TPP model	1-2	1.64	0.39
	3-4	5.04	0.22

Table 2: Comparison of eigenfrequencies of the CD model and flapping dynamics fitted models. The first pole-pair has almost the same eigenfrequency between the two models, which means that in the lower frequencies both models respond comparable. However, the higher eigenfrequency of the flapping dynamics model is not present in the CD model, which explains why high-frequency dynamics are completely damped out in these simulations, as shown in Figure 7.

	Axis	TPP model	CD model
Chirp	p	77.8	77.2
	q	77.3	25.9
Doublets	p	77.6	76.7
	q	64.7	20.0

Table 3: Comparison of NRMSE percentage as given in Equation (10). For both the chirp and doublet value the roll response of both models is similar, but the pitch response matches measurements much better with the TPP model. Still, the pitch response is not perfect, as can also be seen in the doublet time response in Figure 4. The chirp rows show the NRMSE percentage for two pitch and two roll chirps combined while the doublets rows for two pitch and two roll doublets.

in model parameter between the two sets of chirps was 7.7%, but the eigenfrequencies and damping ratios of the systems differ at most 0.9% and 1.8% respectively.

4.3 Parameter RPM dependence

As stated in Section 2, the dependence of the parameters on RPM has been made explicit in the system identification model. Therefore the remaining identifiable parameters should remain constant for different RPMs. A range of RPMs between 1500 and 1650 was tested, and the parameters, which should stay constant, change up to 185% with many parameters changing tens of percentage points. To analyse how the actual model characteristics have changed, the RPM parameter Ω is changed to 1650 RPM in the A- and B-matrices of the model fitted on the 1500 RPM data. If the theoretical relations are correct, the resulting eigenfrequencies and damping should be equal to the model fitted directly on the 1650 RPM chirp data. In reality, the largest eigenfrequency change was 4%, while the largest damping ratio change is 28%, making the model response substantially different from expected. The model fitted on 1500 RPM yielded NRMSE percentages of 72.4% and 67.1% for roll and pitch axes respectively, when tested on the same chirp signal as used in Table 3. Multiple controllers based on models at different RPMs would proba-

Param	Value	CD	Value
A_b	−1.338	L_p	−2.056
B_a	1.448	M_p	10.536
L_b	147.548	L_q	−7.900
M_a	713.378	M_q	−4.777
τ_f	0.091	L_{lat}	−5.361
A_{lat}	−0.282	M_{lat}	−67.573
A_{lon}	0.296	L_{lon}	9.917
B_{lat}	0.524	M_{lon}	11.136
B_{lon}	−0.050		

Table 4: The fitted values for the TPP and CD models. The variables are those given in Equations (5), (6), (8) and (9), while for the TPP model the variables have been made dependent on the RPM again by using the substitutions $\tau_f = \tau_{f_n}/\Omega$, $A_b = A_{b_n}/\Omega^2$ and $B_a = B_{a_n}/\Omega^2$.

bly be needed to accurately control the DelftaCopter. Further research is thus needed to obtain models that generalize well with different rotor RPMs.

4.4 Conclusion

It is clear that the TPP model is much more accurate than the CD model for the DelftaCopter. The extra complex eigenfrequency pair allows better dynamics resolution at higher frequency. Validation doublets confirm this result.

5 RATE CONTROL IN HOVER

In order to further test the validity of the model, a rate controller was designed using standard control techniques and tested. Since the a and b angles are not measured, a linear observer was used to estimate these states in real time, of the form as given in Equation (11). $\hat{x}$ is the current state estimate and L is the correction matrix. The A, B and C matrices are as given in Equations (5) to (7).

$$\dot{\hat{x}} = A\hat{x} + B\bar{u} + L(\bar{y}_{measured} - \hat{y}) \quad (11)$$

$$\hat{y} = C\hat{x} + D\bar{u} \quad (12)$$

The L matrix is chosen using pole placement, setting the poles of the observer at $(-50, -50, -51, 51)$. This is small enough to add some damping to the vibrations caused by the rotor on the gyroscope readings.

The controller is designed using the feedback law given in Equation (13), adding the reference attitude rate $\bar{y}_{ref}$ multiplied by the steady-state gain of the controlled system g, which is given in Equation (14).

$$\bar{u} = -K\hat{x} + g\bar{y}_{ref} \quad (13)$$

$$g = (C(-A + BK)^{-1})^{-1} \quad (14)$$

The gain matrix K is chosen using LQR. This technique finds the optimal gain matrix K for the system minimizing a cost function of state and inputs. The cost matrices of the

LQR design were chosen such that the a and b state cost is very low at 0.001, since these states are not important to the end goal of stabilizing and controlling the attitude rate. The p and q states were given equal cost, fixed at 1. Controllers were then designed for different costs of the system inputs, yielding controllers that are more or less aggressive depending on the input cost. The lower the cost on the input, the faster the controller steers the system, up to the point where input lag and delay makes the response oscillatory and unstable. The input cost of 5 made the system the fastest without introducing these oscillations. The controlled system response is shown in Figure 5. It can be seen that the roll response is delayed, but the measurement follows the command quite well. The pitch response shows a coupling when larger roll rates are present. The pitch response signal is also larger in magnitude than the commanded rates.
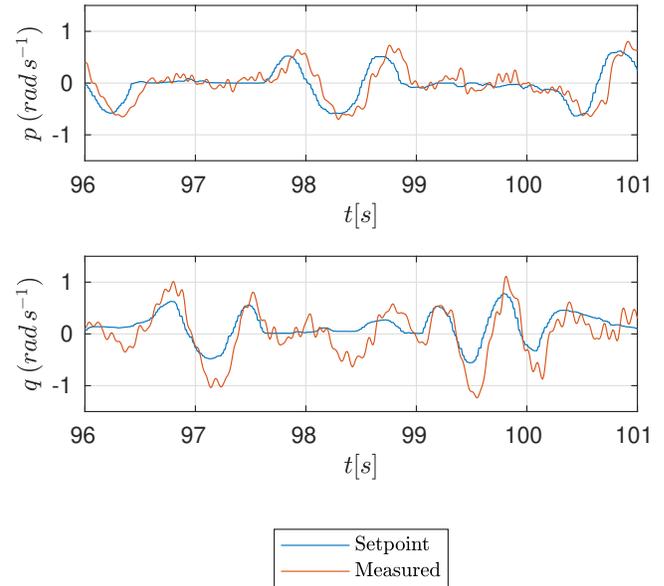

Figure 5: Controller performance during a piloted flight. The pilot directly commands the attitude rate. The roll response is delayed with respect to the command but otherwise has adequate tracking performance. The pitch rate shows coupling with the roll and the response shows larger values than the commands.

The fact that standard control techniques can be used to design a controller for the DelftaCopter, confirms that the TPP model is applicable. While the response is not perfect, the controller is able to stabilize the DelftaCopter without other tuning parameters.

6 FORWARD FLIGHT MODELING

In forward flight, the DelftaCopter pitches down 90° such that the wings are level with the ground. The airspeed increases and the wings generate the required lift to maintain altitude, while the main rotor head is now providing thrust for the aircraft. This means that the aerodynamic surfaces play a

6

significant role in the balance of forces and moments of the DelftaCopter. To be able to design a controller for this flight mode, the TPP and CD hover models were extended. During the forward flight mode, the roll angle of the DelftaCopter in hover mode constitutes a yaw angle in the traditional aircraft sense, but is still referred to as roll. Roll rate (yaw rate in standard aircraft reference frames) is still denoted p. In order to come to a linear model, linear aerodynamic moments are assumed. The model is fitted on forward flight data and a conclusion is drawn on how significant the parameters are.

First of all, the DelftaCopter has four movable surfaces that together supply the role of aileron and elevator where every surface deflection is a linear combination of the aileron and elevator commands. The aileron applies moments to the fuselage along the axis of rotation of the rotor, and as such does not induce coupling on the pitch and roll axes. The elevator does induce a moment on the pitch rate and is thus included in the model with parameter M_{elev}. The short-period longitudinal damping due to a pitch rate M_q and lateral side-slip damping due to a roll rate L_p are included. In the CD model, they are lumped into the parameters already present, while in the TPP model these damping parameters are not yet present and are added. The resulting $A_{TPP,FW}$ and $B_{TPP,FW}$ matrices for forward flight are given in Equations (15) and (16). The state vector is the same as for the hover vector while the input vector now is $\bar{u} = (\delta_x, \delta_y, \delta_e)^T$.

$$A_{TPP,FW} = \begin{bmatrix} L_b & 0 & 0 & L_b \\ 0 & M_q & M_a & 0 \\ 0 & -1 & -\frac{\Omega}{\tau_{fn}} & \frac{A_{b_n}}{\Omega\tau_{fn}} \\ -1 & 0 & \frac{B_{a_n}}{\Omega\tau_{fn}} & -\frac{\Omega}{\tau_{fn}} \end{bmatrix} \quad (15)$$

$$B_{TPP,FW} = \begin{bmatrix} 0 & 0 & 0 \\ 0 & 0 & M_{elev} \\ \frac{A_{lat}\,\Omega}{\tau_{fn}} & \frac{A_{lon}\,\Omega}{\tau_{fn}} & 0 \\ \frac{B_{lat}\Omega}{\tau_{fn}} & \frac{B_{lon}\Omega}{\tau_{fn}} & 0 \end{bmatrix} \quad (16)$$

L_p and M_q represent aerodynamic damping on the roll and pitch rate. As before, the parameters L_b and M_a of the TPP model are the representative spring constants, and their physical meaning is given by Mettler[2, sec. 3.1], with M_a for example given in Equation (17). This relates the TPP angle to the angular acceleration of the fuselage, and contains a rotor stiffness term and a thrust term. The rotor blade spring stiffness k_β is equal to $88\,\mathrm{N\,m\,rad}^{-1}$[1], which is much higher than the thrust contribution at maximum weight $hT \approx hmg \approx 0.15 \cdot 4.5 \cdot 9.81 = 6.6\,\mathrm{N\,m\,rad}^{-1}$. Therefore, while the thrust may become smaller in forward flight, the parameters L_b and M_a are assumed constant in fitting the forward flight models.

$$M_a = \frac{k_\beta + hT}{I_{yy}} \quad (17)$$

The flight test used to fit the parameters is a forward flight test in level flight. The airspeed fluctuates between $17\,\mathrm{m\,s}^{-1}$ and $19.5\,\mathrm{m\,s}^{-1}$, while the RPM fluctuates between 1550 and 1720. This RPM range is quite broad compared to the hover experiments, especially considering the observed sensitivity of parameters to the RPM.

The parameters of the TPP and CD models are given in Table 5. Comparing these to the hover parameters as given in Table 4 shows that the hover and forward flight models have comparable parameters for the rotor dynamics in the TPP model case. It seems that the roll rate damping is very small, which is logical since the vertical stabilizer has a small moment arm to the center of mass.

TPP	Value	CD	Value
A_{b_n}	-0.908	L_p	-10.690
B_{a_n}	0.999	M_p	14.899
L_b	147.550	L_q	-9.251
M_a	713.380	M_q	1.050
τ_{f_n}	0.075	L_{lat}	6.605
A_{lat}	-0.196	M_{lat}	-70.459
A_{lon}	0.214	L_{lon}	-2.903
B_{lat}	0.440	M_{lon}	11.532
B_{lon}	-0.026	M_{elev}	10.263
L_p	-0.930		
M_q	4.691		
M_{elev}	37.752		

Table 5: The fitted values for the TPP and CD models in forward flight. The variables for the TPP model have been made dependent on the RPM again by using the substitutions $\tau_f = \tau_{f_n}/\Omega$, $A_b = A_{b_n}/\Omega^2$ and $B_a = B_{a_n}/\Omega^2$. The $A_{TPP,FW}$ and $B_{TPP,FW}$ matrices of the forward TPP model are given in Equations (15) and (16). The CD model $A_{cyl,FW}$-matrix is the same as Equation (8), while the $B_{cyl,FW}$ matrix is as given in Equation (8), with the addition of a third input, elevator δ_{elev} linearly related to pitch acceleration $\dot{q}$ through parameter M_{elev}.

In Figures 8 to 10 the models are simulated on measurements of forward flight data, on roll, pitch and elevator chirps respectively. This chirp data was not used for fitting the parameters and can be used for validation. It is clear that the TPP model is better at predicting the high-frequency response than the CD model, but the fit is not as good as on the hover mode. This can be due to the RPM fluctuations or the TPP model not being applicable to the high rotor inflow experienced in forward flight. Another cause of model inaccuracy could be aerodynamic effects missing in the model. The angle of attack is not part of the model and was not measured, but could have an important influence. Surprisingly, the M_q parameter is positive, implying a positive feedback loop on the pitch rate. This could be due to the missing other influences in the model. The accuracies of the models can be seen

in Table 6.

	Axis	TPP model	CD model
Fitting	p	66.0	70.8
	q	54.7	21.7
Validation	p	49.7	53.1
	q	47.1	17.0

Table 6: Comparison of NRMSE percentage as given in Equation (10) for forward flight. Both fitting and validation percentages concern three chirps, one roll, one pitch and one elevator. Simulation of the models on the validation chirps can be found in Figures 8 to 10.

7 CONCLUSION

In order to design a new controller for the DelftaCopter, a new modeling approach was required that better captures the attitude dynamics. A system identification modeling approach was chosen and two models were compared: the previously used Cylinder Dynamics (CD) model which assumes a rigid rotor[1], and a Tip-Path Plane (TPP) model which was derived by Mettler[2]. Chirps were used as system identification maneuver and the models were compared. It is clear from Section 4 that the TPP model is much better at generating the high-frequency response than the CD model. This is validated using manually flown doublets, for which the TPP response also shows better accuracy. To show that this model is usable for control design, an attitude rate controller is designed using the standard LQR technique, with reasonable control response as shown. It can thus be concluded that the flapping dynamics have a significant influence on the attitude dynamics of the DelftaCopter.

The relationship between the identified parameters and rotor RPM was found to be different than predicted from theory. This may be due to the lumping together of unmodeled effects into the present parameters. Probably models at different RPMs are required for accurate control at these different RPMs.

For forward flight, the TPP model was extended to include roll rate and pitch rate damping, while both the TPP model and CD model include a constant for the elevator effectiveness. It is shown that the hover model with this extension is applicable to forward to some extent.

8 RECOMMENDATIONS

The following recommendations are made on what research could be conducted next:

- Measure the a and b states in flight to give more accurate models and validate the current model's prediction.

- Investigate the TPP model's parameters' dependence on RPM to broaden the accurate flight envelope of the model.

- Measure more aircraft states in forward flight, to allow the attitude dynamics model to depend on, in particular, angle of attack. Generalize the forward flight model for different airspeeds and RPMs.

- Use the forward flight model for attitude control.

REFERENCES

[1] Christophe De Wagter and Ewoud J.J. Smeur. Control of a hybrid helicopter with wings. *International Journal of Micro Air Vehicles*, 9(3):209–217, sep 2017.

[2] Bernard Mettler. *Identification Modeling and Characteristics of Miniature Rotorcraft*. Springer US, Boston, MA, 2003.

[3] S Herbst, G Wortmann, and M Hornung. Conceptual design studies of vertical takeoff and landing remotely piloted aircraft systems for hybrid missions. *CEAS Aeronautical Journal*, 7:135–148, 2016.

[4] Menno Hochstenbach, Cyriel Notteboom, Bart Theys, and Joris De Schutter. Design and Control of an Unmanned Aerial Vehicle for Autonomous Parcel Delivery with Transition from Vertical Take-off to Forward Flight -VertiKUL, a Quadcopter Tailsitter. *International Journal of Micro Air Vehicles*, 7(4):395–405, 2015.

[5] Atsushi Oosedo, Satoko Abiko, Atsushi Konno, Takuya Koizumi, Tatuya Furui, and Masaru Uchiyama. Development of a quad rotor tail-sitter VTOL UAV without control surfaces and experimental verification. In *2013 IEEE International Conference on Robotics and Automation*, pages 317–322. IEEE, may 2013.

[6] B. Bataillé, J.-M. Moschetta, D. Poinsot, C. Bérard, and A. Piquereau. Development of a VTOL mini UAV for multi-tasking missions. *The Aeronautical Journal*, 113(1140):87–98, feb 2009.

[7] L.R. Lustosa, F. Defay, and J.M. Moschetta. Development of the flight model of a tilt-body MAV. In *IMAV*, jan 2014.

[8] M Bronz, EJ Smeur, and HG de Marina. Development of A Fixed-Wing mini UAV with Transitioning Flight Capability. *35th AIAA Applied*, 2017.

[9] Christophe De Wagter, Rick Ruijsink, Ewoud Smeur, Kevin van Hecke, Freek van Tienen, Erik van der Horst, and Bart Remes. Design, Control and Visual Navigation of the DelftaCopter. jan 2017.

[10] UAV Challenge. UAVC Medical Express 2018 Rules V2, 2017.

[11] Konstantin Kondak, Markus Bernard, Nikolas Losse, and Günter Hommel. Autonomously Flying VTOL-Robots: Modeling and Control. In *Proceedings 2007 IEEE International Conference on Robotics and Automation*, pages 736–741. IEEE, apr 2007.

[12] A.R.S. Bramwell, G. Done, and David. Balmford. *Bramwell's Helicopter Dynamics*. American Institute of Aeronautics and Astronautics, 2001.

[13] Bernard Mettler, Chris Dever, and Eric Feron. Scaling Effects and Dynamic Characteristics of Miniature Rotorcraft. *Journal of Guidance, Control, and Dynamics*, 27(3):466–478, may 2004.

[14] Konstantin Kondak, Markus Bernard, Nikolas Losse, and Günter Hommel. Elaborated modeling and control for autonomous small size helicopters. In *Proc. ISR/ Robotik*, 2006.

[15] Subodh Bhandari, Richard Colgren, Philipp Lederbogen, and Scott Kowalchuk. Six-DoF dynamic modeling and flight testing of a UAV helicopter. *AIAA Modeling and Simulation Technologies Conference and Exhibit*, (August):992–1008, 2005.

[16] Luis A Sandino, Manuel Bejar, Anibal Ollero, L A Sandino, A Ollero Grvc, M Bejar, and A Ollero. A Survey on Methods for Elaborated Modeling of the Mechanics of a Small-Size Helicopter. Analysis and Comparison. *Journal of Intelligent & Robotic Systems*, 72:219–238, 2013.

[17] Mark B Tischler and Robert K. Remple. *Aircraft and Rotorcraft System Identification: Engineering Methods with Flight Test Examples*. 2008.
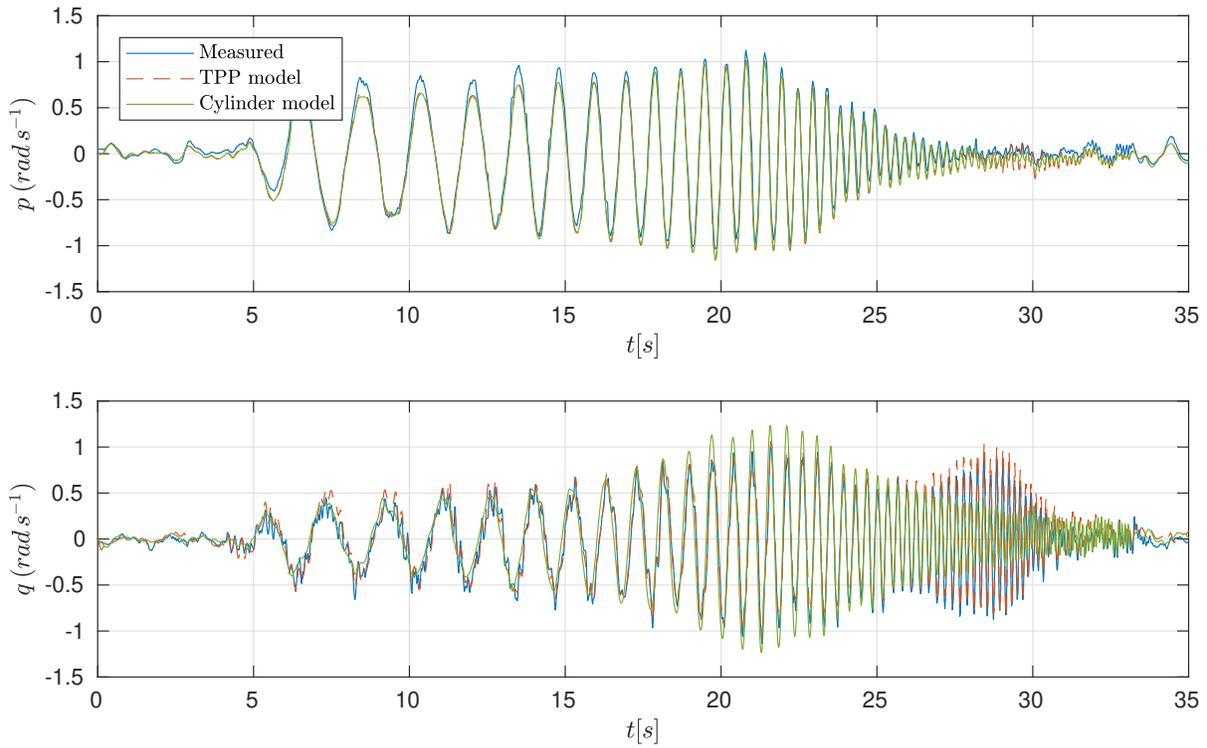
APPENDIX A: CHIRP MEASUREMENTS

Figure 6: Chirp on the roll axis in hover. The pitch motions are mainly due to pitch-roll coupling. The TPP model is much better at producing the measured pitch signals in the higher frequency range.
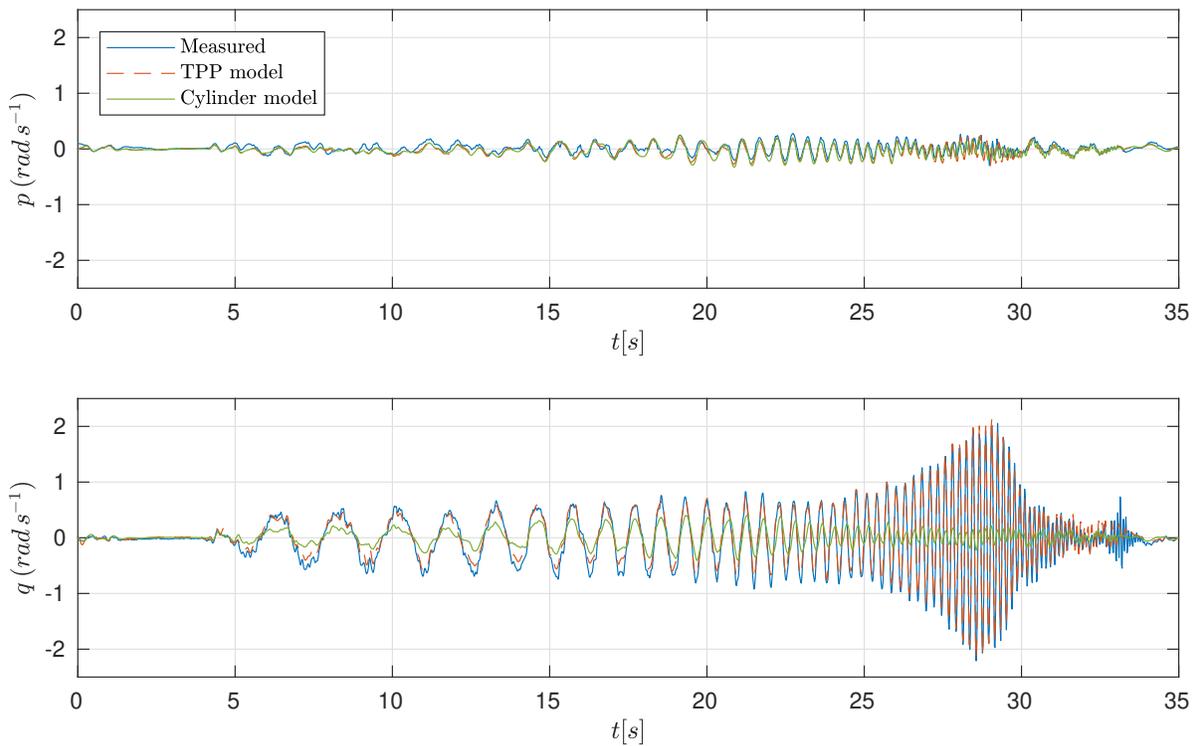

Figure 7: Chirp on the pitch axis in hover. The roll motion due to pitching is much less severe due to the high roll inertia compared to the pitch inertia. Now the CD model's accuracy at low frequencies is also worse than the TPP model.
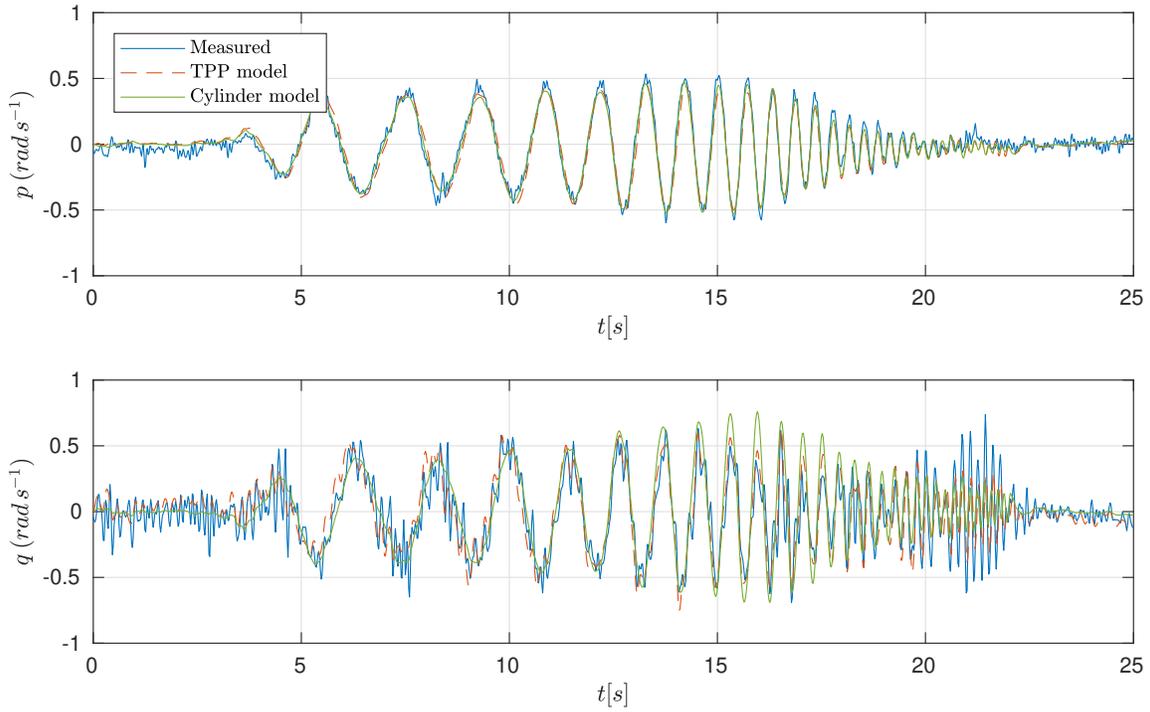
Figure 8: Validation chirp on the roll axis in forward flight. The pitch motions are probably mainly due to pitch-roll coupling. The TPP and CD model have a similar response. The high-frequency fluctuations in the pitch response are due to the attitude controller which is active during the chirp.
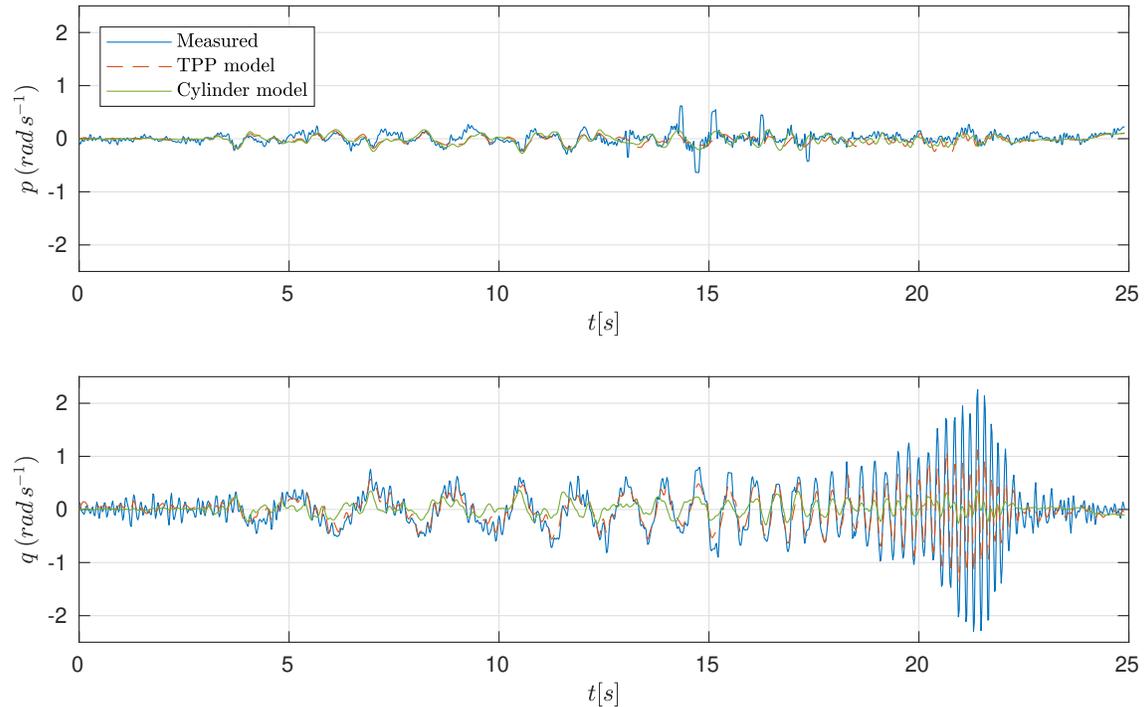

Figure 9: Validation chirp on the pitch axis in forward flight. The CD model's accuracy is much worse than the TPP model, while the latter is also unable to follow the measurement signal at higher frequencies. At around $15\,\mathrm{s}$, the logging system shows some delays, leading to dropped measurements.
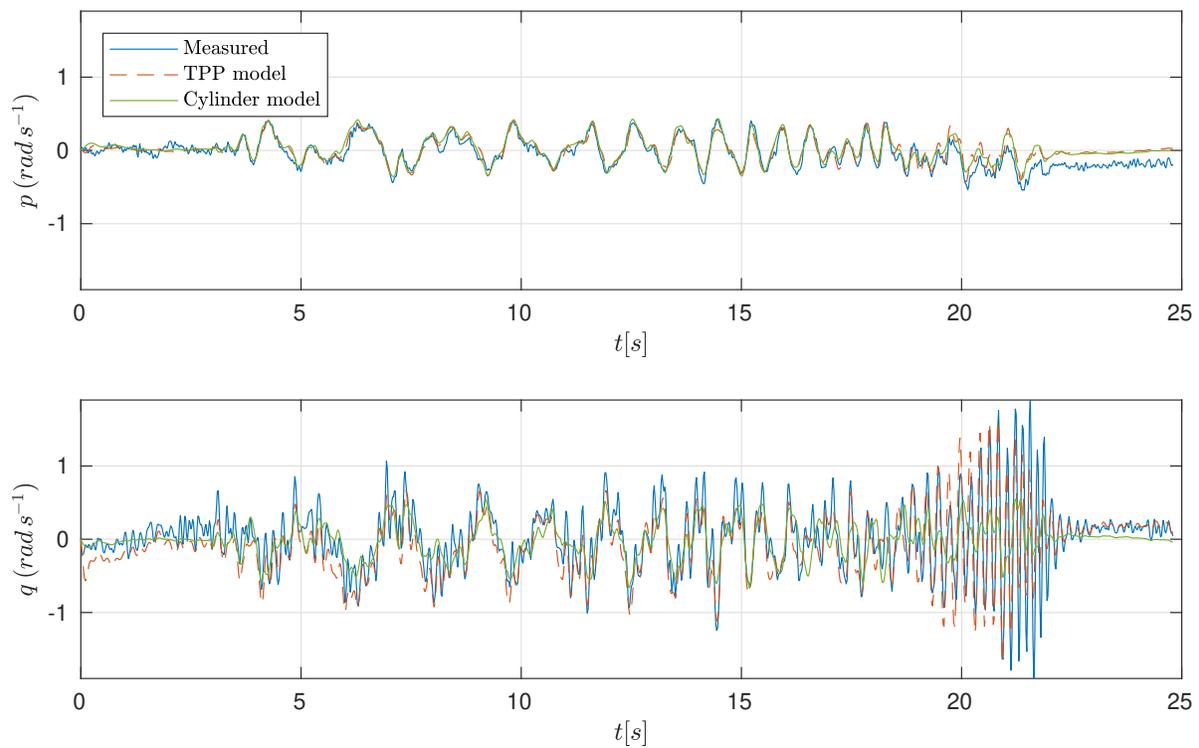
Figure 10: Validation chirp on the elevator axis in forward flight. The roll response q (yaw in standard aircraft reference frame) is fitted accurately by both TPP and CD models, while from around $15\,\mathrm{s}$ the CD model is unable to replicate the higher frequencies that the TPP model can still generate. The TPP model is still unable to replicate the highest frequencies of the chirp.